

Spray Deposition and Characterization of p-type Li doped NiO Thin Films

S. Mani Menaka^{1,*}, G. Umadevi² and A. Uma Maheswari²

¹ Research and Development Centre, Bharathiar University, Coimbatore - 641046, Tamilnadu, India.

² PG and Research Department of Physics, Government Arts College, Coimbatore - 641018, Tamilnadu, India.

Received: 2 Jun. 2018, Revised: 2 Aug. 2018, Accepted: 20 Aug. 2018.

Published online: 1 May 2019.

Abstract: Undoped and lithium doped nickel oxide (Li doped NiO) thin films have been prepared onto glass substrates at 450 °C by chemical spray pyrolysis technique. The effect of lithium (Li) concentrations on the structural, optical, photoluminescence and electrical properties of the Li doped NiO films were studied by X-ray diffraction (XRD), UV-vis-NIR spectrophotometer, Photoluminescence (PL) spectrophotometer, Hot probe and Hall effect measurement system. The PL results confirmed that the band gap reduces when the lithium concentration increases. The structural properties of undoped and Li doped NiO films showed polycrystalline cubic structure. The optical transmittance and band gap values of the films decreases, while the absorption values increases with the increase in Li concentration. Moreover, it has been observed that the resistivity of the above films decreases with the increase in Li concentration.

Keywords: Spray pyrolysis; Nickel oxide; Lithium doped; Polycrystalline; Band gap; Resistivity.

1 Introduction

Transparent conducting oxides (TCOs) have been extensively studied in recent years since they exhibit high optical transparency and high electrical conductivity. TCO thin films are used in various applications such as solar cells, light emitting diodes, and electrochromic devices. Widely known TCO thin films such as ITO, FTO, SnO₂, and ZnO are only n-type semiconductors. However p-type conducting films are required for the devices where hole injection is required. Such p-type transparent semiconductors are relatively rare. NiO is one of a p-type semiconducting material with wide band gap of 3.6 - 4 eV [1]

There are a number of physical and chemical routes for preparing NiO thin films, like chemical bath deposition [2], chemical vapor depositions [3], pulsed laser deposition [4], thermal evaporation [5], vacuum evaporation [6], RF magnetron sputtering [7], Ion beam sputtering [8], sol-gel process [9], and spray pyrolysis [10, 11]. Among these, the spray pyrolysis technique is unique, reproducible, simple, low cost, safe, allow doping of different elements and deposition onto large-areas without the need for vacuum and versatile method for synthesis of thin films.

NiO has been considered as a promising material with

possible applications in different fields, such as smart windows [12], antiferromagnetic layer [13], photodetectors [14], catalysts [15], electrochromic devices [16], heterojunction solar cells [17], chemical sensors [18].

In this present work, the influence of concentration on the structural, optical, and electrical properties of undoped and Li doped NiO thin films deposited by spray pyrolysis technique is considered.

2 Experimental

2.1 Materials Synthesis

Undoped and Li doped NiO thin films were prepared using nickel chloride hexahydrate (NiCl₂·6H₂O) and lithium chloride monohydrate (LiCl·H₂O) as the starting materials. The isopropyl alcohol was added in a solution to reduce the surface tension on glass substrate. The films were deposited onto glass substrates using the spray pyrolysis technique which were chemically and ultrasonically cleaned before deposition. During the film deposition the substrate temperature was kept constant at 450 °C. For deposition of undoped films, 0.1 M of NiCl₂·6H₂O was dissolved in distilled water to make precursor solution. For deposition of Li doped NiO films, the precursor solution was prepared by

*Corresponding author E-mail: anisulme11@gmail.com

dissolving $\text{NiCl}_2 \cdot 6\text{H}_2\text{O}$ and different concentrations (2%, 4% and 8%) of $\text{LiCl} \cdot \text{H}_2\text{O}$ in distilled water. The optimized conditions were arrived at the following parameters: spraying time (5 sec), spray interval (2 min), deposition rate (8 ml/min), pressure of the carrier gas (1.5 bar) and spray nozzle-substrate distance (30 cm) were kept constant for each concentration.

2.2 Materials Characterization

A 'Rigaku' X-ray diffractometer (XRD) with a $\text{CuK}\alpha$ radiation ($\lambda = 1.5418 \text{ \AA}$) was used for structural studies in the range of $2\theta = 10-90^\circ$. The optical transmittance and the absorbance spectra of the films were taken from a 'Perkin Elmer Lambda' UV-Vis-NIR spectrophotometer in the range of $200-2400 \text{ cm}^{-1}$, and then the optical band gap of the films were calculated using the optical method. The photoluminescence (PL) spectra of the NiO films were recorded using a 'Varian Cary Eclipse Fluorescence Spectrophotometer'. The majority carrier type of the as-deposited films were carried out by the Hot probe technique and Hall effect system. The electrical resistivity of the films were measured by the 'Ecopia HMS 5000' Hall effect measurement system.

3 Results and discussion

3.1 Structural Properties

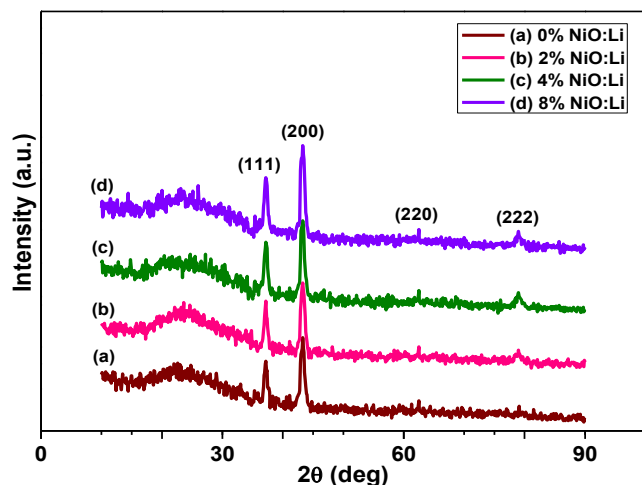


Fig.1: XRD of undoped and Li doped NiO thin films.

The XRD patterns of NiO corresponding to different doping concentrations of Li (0% to 8%) were shown in Fig.1. The undoped and Li doped NiO films in the range between 10° and 90° were analyzed by XRD technique to study the structural identification and changes in the crystalline.

Only peaks corresponding the (111), (200), (220) and (222) directions are visible and all the peaks visible belong to the cubic NiO phase (JCPDS 04-0835). It is found that both the undoped and Li doped NiO film samples are polycrystalline,

comprising a strong reflection along (200) plane, medium reflection along (111) plane and a weak reflection along (220) and (222) planes. The intensity of the peaks corresponding to the (111) and (200) planes increases as the Li concentrations increases from 0% to 8%. The positions of the peaks and the presence of more than one diffraction peak lead to the conclusion that the films are polycrystalline in nature with a cubic crystalline structure. The crystallite size (D) as predicted by the well-known Scherrer's formula [19] is:

$$D = \frac{k\lambda}{\beta \cos \theta} \quad (1)$$

where k is the dimensionless number equal to 0.9, λ is the X-ray wavelength, β is the full width at half maximum (FWHM) of diffraction peak and θ is the Bragg diffraction angle.

The lattice parameter (a) can be evaluated from the relation [20]:

$$a = d_{hkl} \sqrt{h^2 + k^2 + l^2} \quad (2)$$

where d_{hkl} is the inter-plane spacing, and h , k & l are the indices of the planes.

The variation of lattice constant and crystallite size of the films were shown in Fig.2 and listed in Table 1. The lattice parameter for (200) plane varies from 0.4186 nm to 0.4184 nm for the different Li concentrations (0% to 8%). The average lattice parameter for (200) plane is found to be 0.4185 nm which is very close to the standard value for bulk NiO taken from JCPDS file no. 04-0835. As the Li concentration increases, a notable change in lattice parameter was not observed. This is due to the slight variation of ionic radius of Li^+ (0.76 Å) compared to that of Ni^{2+} (0.69 Å).

In addition, the increase in the intensity of the peaks may be attributed to the grain growth associated with the increase in the crystallite size by increasing the Li concentration. The crystallite size of the films for (200) plane increases from 17.86 nm to 21.43 nm as the Li concentration increases from 0% to 8%. This is due to improved crystalline quality of the films. The average crystallite size of the pure NiO and Li:NiO films for (200) plane is 19.12 nm.

3.2 Optical Properties

3.2.1 Transmittance

The optical transmittance curves as a function of wavelength at different concentrations were plotted in Fig.3. The optical transmittance spectra of the undoped and Li doped NiO thin films which were recorded in the wavelength range of 200-2400 nm. It can be seen that the undoped and Li doped NiO films having a higher transmittance in the visible-near infrared (Vis-NIR) regions, while the transmittance in the UV region is very low. The highest transmittance value of pure NiO film is 60% and 70% in the Vis and NIR regions. The transmittance of Li doped NiO decreases to about 40% and

53% in the Vis and NIR regions when the Li concentration increases from 0% to 8%. This results may be ascribed to the light being scattered by large amounts of grain

boundaries as well as the Li clusters also reflecting the incident light, therefore the transmittance of Li doped NiO films decreases with the increase in Li concentration

Table 1: Structural parameters for undoped and Li doped NiO thin films.

Lithium concentration (%)	2 θ (°) for (200)	FWHM (°) for (200)	Lattice parameter (nm)	Crystallite size of XRD (nm)
0	43.40	0.4833	0.4186	17.86
2	43.41	0.4750	0.4186	18.09
4	43.42	0.4583	0.4184	19.08
8	43.43	0.4000	0.4184	21.43

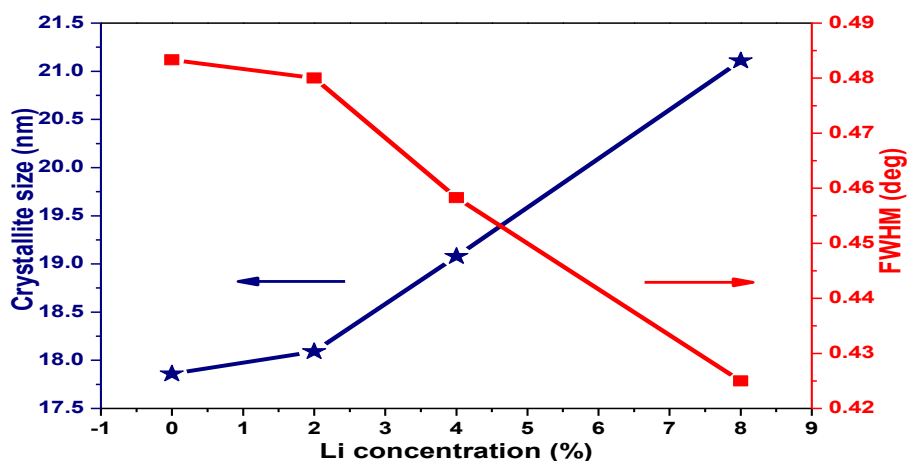


Fig.2: The variations of lattice constant and crystallite size of undoped and Li doped NiO thin films.

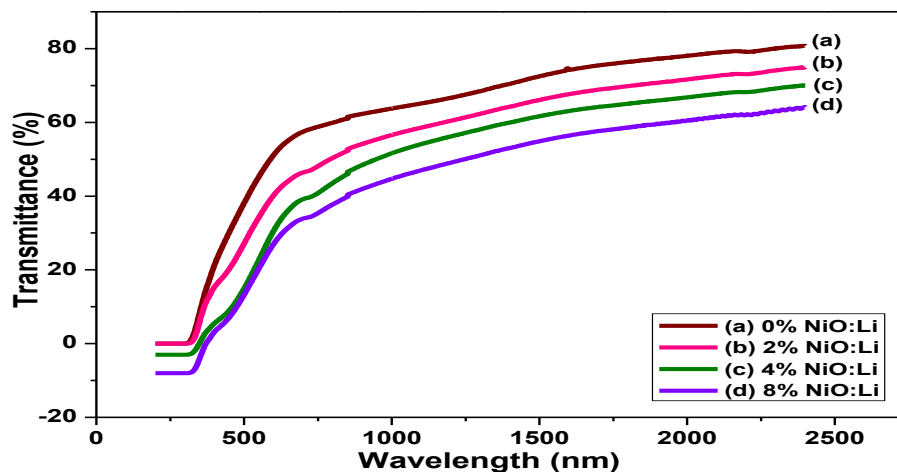


Fig.3: Transmittance versus wavelength of undoped and Li doped NiO thin films

3.2.2 Absorption

Fig.4 shows the optical absorption as a function of wavelength in the range of 200-2400 nm for undoped and Li dopedNiO thin films at different concentrations. It is opposite to that of transmittance spectrum. The undoped and Li dopedNiO films show higher absorption in the UV region, and low absorption in the Vis-NIR regions. It has been observed that the absorbance of undoped and Li dopedNiO increases as the Li concentration increases from 0% to 8%. This evident increase of energy is due to the interaction of the material electrons with the incident photons which have enough energy for the occurrence of electron transitions.

3.2.3 Band Gap

Fig.5 shows the optical band gap for undoped and Li dopedNiO thin films. The optical absorption data were taken to obtain the optical band gap. The absorption coefficient (α) of the films has been calculated from the absorption data using the following relation [21]:

$$\alpha = \frac{2.303 A}{d} \quad (3)$$

where A is the absorption and d is the film thickness.

The band gap of the films is determined by plotting $(\alpha h\nu)^2$ vs $h\nu$ and is expressed as follows [22]:

$$\alpha h\nu = A_0 (h\nu - E_g)^n \quad (4)$$

where α is the absorption coefficient, h is Planck's constant, ν is the frequency of the incident photon, A_0 is an energy-independent constant, E_g is the band gap energy, and n is a number equal to 1/2 for direct band gap and 2 for indirect band gap compound.

The band gap energy is determined from the extrapolated straight line portion of the plot to the x axis, $(\alpha h\nu)^2 = 0$. The linear nature of the plots at the absorption edge confirmed that all deposited films undoped and Li dopedNiO films are semiconductor with direct band gap. The optical band gap of undoped and Li dopedNiO films gradually decreases from 3.94 eV to 3.69 eV with Li concentration.

3.3 Photoluminescence Properties

The photoluminescence (PL) emission spectra at room temperature of undoped and Li dopedNiO thin films deposited at different Li concentrations were shown in Fig.6. It can be seen that the undoped and Li dopedNiO thin films can exhibit obvious excitonic PL signals with similar curve shape, demonstrating that doping with lithium will not generate a different PL phenomena as it is unable to capture electrons. Thus, all spectra exhibit identical emission peaks.

The energy band gap from photoluminescence spectra of the undoped and Li dopedNiO films are calculated by using the following equation [23]:

$$E_g = \frac{1240}{\lambda \text{ (nm)}} \quad (5)$$

The role of surface and native defects has been invoked to explain the observed PL behavior. The PL emission spectrum consist of two emission peaks. For the emission peaks 365 nm and 467 nm the energy band gaps are found to be 3.40 eV and 2.66 eV respectively. From the spectra, it may be observed that the intensities of the PL spectra are decreases with the increase in lithium concentration. A strong PL emission peak found at 365 nm was attributed to the electronic transitions of Ni^{2+} and O^{2-} ions. The second emission peak at 467 nm might be attributed to oxygen related defects.

3.4 Electrical Properties

Electrical resistivity and conductivity for undoped and Li dopedNiO films with various Li doping concentrations were shown in Fig.7 and listed in Table 2. All the NiO films exhibited p-type conductivity as determined by hot probe technique and verified by the sign of the Hall coefficient. The resistivity of the undopedNiO thin film is $3.20 \times 10^2 \Omega \text{ cm}$. The resistivity decrease substantially to $0.56 \times 10^2 \Omega \text{ cm}$ when the Li doping concentration is increase to 8%. As the electrical conductivity is inverse of resistivity, the electrical conductivity increased with Li doping. NiO is a p-type semiconductor due to the Ni^{2+} vacancies. When Li^+ ions ($r_{\text{ion}} = 0.76 \text{ \AA}$) began to substitute for Ni^{2+} ($r_{\text{ion}} = 0.69 \text{ \AA}$) ions in normal crystal site positions, each Li^+ is capable of donating only one electron to the O^{2-} and the excess of uncompensated holes increases the p-type behavior of the films, thereby increasing the carrier concentration with a subsequent decrease in the resistivity value in the Li dopedNiO composite film.

Table 2: Optical and Electrical parameters for undoped and Li dopedNiO thin films.

Lithium concentration (%)	Band gap (eV)	Resistivity ($\times 10^2 \Omega \text{ cm}$)	Conductivity ($\times 10^{-3} \Omega^{-1} \text{ cm}^{-1}$)
0	3.94	3.20	3.13
2	3.78	2.50	4.00
4	3.74	1.74	5.75
6	-	1.08	9.26
8	3.69	0.56	17.86

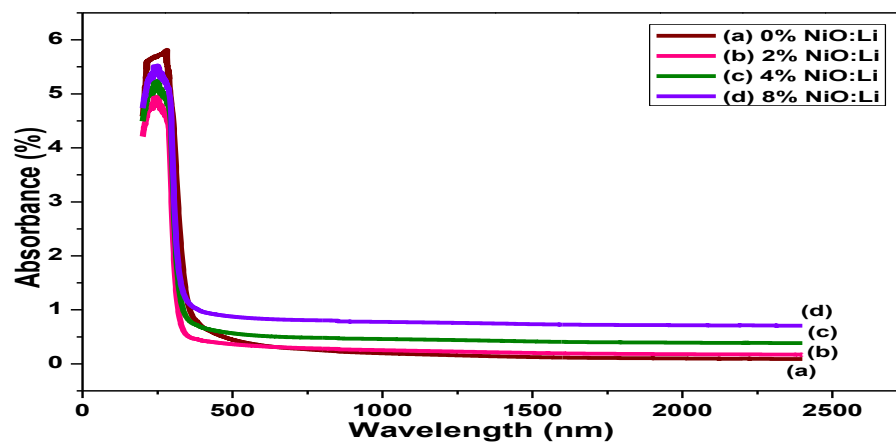


Fig.4: Absorbance versus wavelength of undoped and Li doped NiO thin films.

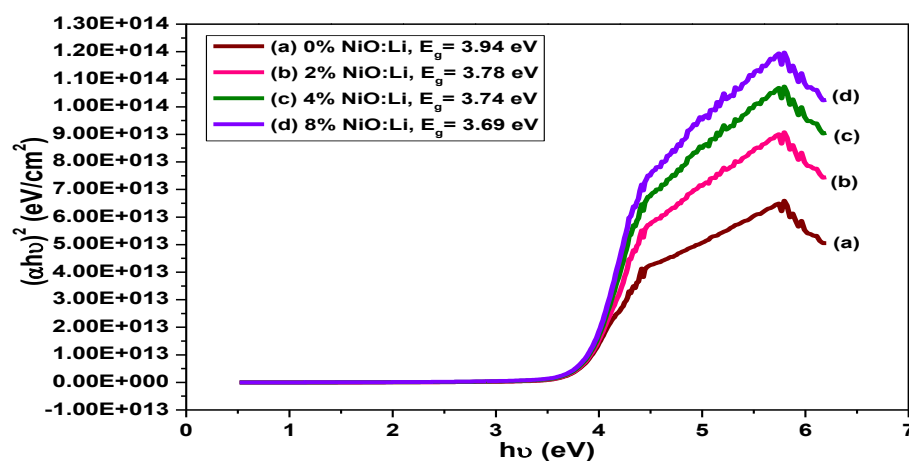


Fig.5: Optical band gap of undoped and Li doped NiO thin films.

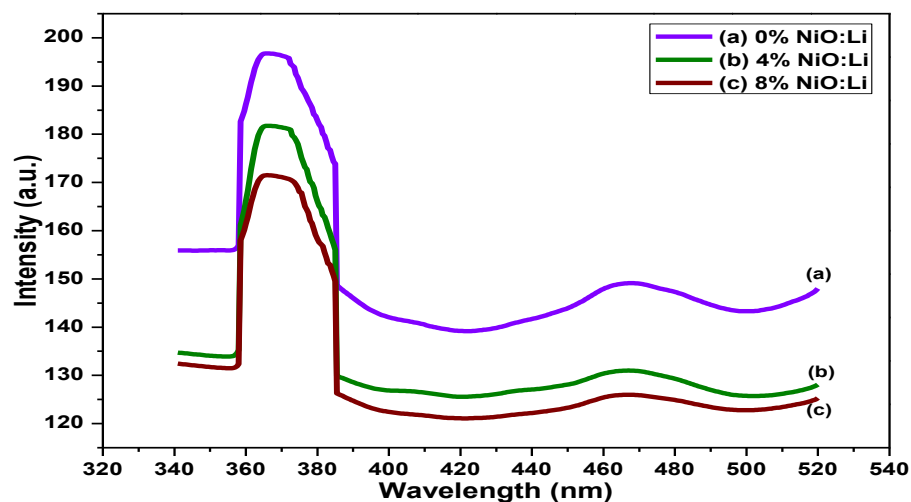


Fig.6: Photoluminescence spectra of the undoped and Li doped NiO thin films

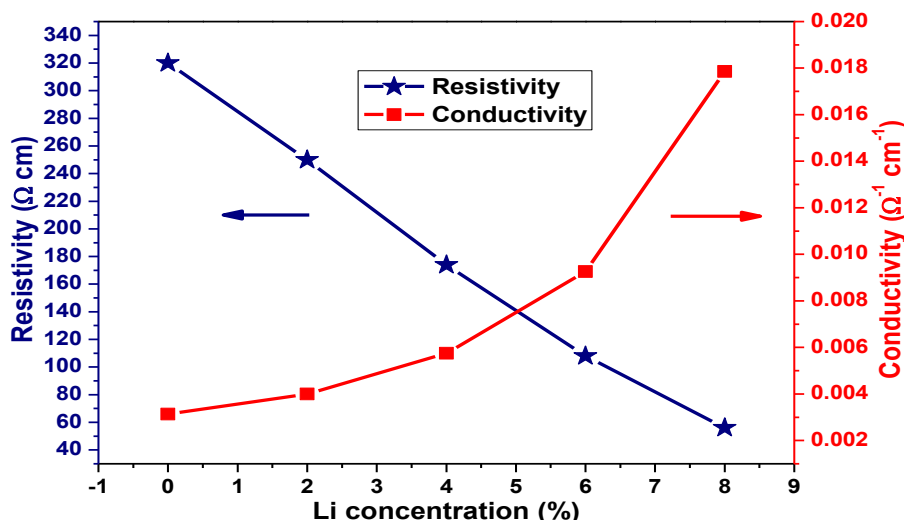


Fig.7: Resistivity and Conductivity of undoped and Li doped NiO thin films.

4 Conclusions

The thin films of undoped and Li doped NiO were prepared by spray pyrolysis technique at different concentrations level onto glass substrate. The effects of the Li doping concentration on the structural, optical, photoluminescence, and electrical properties of all the films were studied. The XRD results show that all the films have been found to show cubic polycrystalline structure. The average lattice parameter of the undoped and Li doped NiO films for (200) plane is found to be 0.4185 nm which is very close to the standard value. The crystallite size of the films increases from 17.86 nm to 21.43 nm with the increase in Li concentration from 0% to 8%. The optical band gap decreases from 3.94 eV for a undoped NiO film to 3.69 eV after 8% addition of Li for NiO film. Band gap of the thin films are estimated as 3.40 eV and 2.66 eV using Photoluminescence. The resistivity decreases from 3.20×10^2 to $0.56 \times 10^2 \Omega \text{ cm}$ with increase in Li doping Concentrations level in NiO. These values are reasonable for p-type TCOs.

References

- [1] P.S. Patil and L.D. Kadam, Appl. Surf. Sci., **199**, 211-221, 2002.
- [2] L. Barkat, L. Cattin, A. Reguig, M. Regragui, J.C. Bernède, Mater. Chem. Phys., **89**, 11, 2005.
- [3] W.C. Yeh, M. Matsumura, Jpn. J. Appl. Phys., **36**, 6884-6887, 1997.
- [4] D. Franta, B. Negulescu, L. Thomas, P.R. Dahoo, M. Guyot, I. Ohlídal, J. Mistrík, T. Yamaguchi, Appl. Surf. Sci., **244**, 426-430, 2005.
- [5] M. Dinescu, P. Verardi, Applied Surface Science., **106**, 149-158, 1996.
- [6] R. Tsu, L. Esaki, R. Ludeke, Phys. Rev. Lett., **23**, 977, 1969.
- [7] Y. Ushio, A. Ishikawa, T. Niwa, Thin Solid Films., **280**, 233, 1996.
- [8] J. Peng, Z. Xu, S. Wang, Q. Jie, C. Chen, Sensors and Materials., **22**, 409-416, 2010.
- [9] A. Alshahrie, Superlattices and Microstructures., **96**, 75-81, 2016.
- [10] B.A. Reguig, A. Khelil, L. Cattin, M. Morsli and J.C. Bernède, Applied Surface Science., **253**, 4330-4334, 2007.
- [11] U.P. Muecke, N. Luechinger, L. Schlagenhauf, L.J. Gauckler, Thin Solid Films., **517**, 1522-1529, 2009.
- [12] R. Romero, F. Martin, J.R. Ramos-Barrado, D. Leinen, Thin Solid Films., **518**, 4499-4502, 2010.
- [13] E. Fujii, A. Tomozawa, H. Torii, R. Takayama, Journal of Applied Physics., **35**, L328-330, 1996.
- [14] Leong-M. Choi, I.M. Seongil, Applied Surface Science., **244**, 435-438, 2005.
- [15] A.K. Roslik, V.N. Konev, and A.M. Maltsev, Oxidation of Metals., **43**, 1, 1995.
- [16] S.H. Lin, F.R. Chen, J.J. Kai, Appl. Surf. Sci., **254**, 3357, 2008.
- [17] C.H. Pandis, N. Brilis, E. Bourithis, D. Tasamakis, Ali H. Krishnamoorthy et al., IEEE Sens. J., **7**, 448-454, 2007.
- [18] H. Kumagai, M. Matsumoto, K. Toyoda, M. Obara, J. Mater. Sci. Lett., **15**, 1081-1083, 1996.
- [19] H.P. Klug, L.E. Alexander, X-ray Diffraction Procedures for Polycrystalline and Amorphous Materials, Wiley, New York, 1974.
- [20] Y.M. Lu, W.S. Hwang, J.S. Yang, H.C. Chuang, Thin Solid Films., **420**, 54-61, 2002.
- [21] Dr Adel, H. Omran Alkhatayatt, Al-Qadisyah, J. Sci., **14**, 76, 2009.
- [22] J.M. Shah, Y.L. Li, T. Gessmann, E.F. Schubert, J. Appl. Phys., **94**, 2627-2631, 2003.
- [23] S.S. Ahmed, E.K. Hassan, G.H. Mohamed, International Journal of advanced research., **2**, 633-638, 2014.